Ocean–Atmosphere Interaction and the Tropical Climatology. Part I: The Dangers of Flux Correction

J. DAVID NEELIN

Department of Atmospheric Sciences, University of California Los Angeles, Los Angeles, California

HENK A. DIJKSTRA

Institute for Marine and Atmospheric Research Utrecht, University of Utrecht, Utrecht, the Netherlands

(Manuscript received 8 February 1994, in final form 5 October 1994)

ABSTRACT

This sequence of papers examines the role of dynamical feedbacks between the ocean and the atmosphere in determining features of the tropical climatology. A stripped-down, intermediate, coupled ocean–atmosphere model is used to provide a prototype problem for the Pacific basin. Here the authors contrast the fully coupled case with the case where flux correction is used to construct the climatology. In the fully coupled case, the climatology is determined largely by feedback mechanisms within the ocean basin: winds driven by gradients of sea surface temperature (SST) within the basin interact with the ocean circulation to maintain SST gradients. For all realistic cases, these lead to a unique steady solution for the tropical climatology. In the flux-corrected case, the artificially constructed climatology becomes unstable at sufficiently large coupling, leading to multiple steady states as found in a number of coupled models. Using continuation methods, we show that there is a topological change in the bifurcation structure as flux correction is relaxed toward a fully coupled case; this change is characterized as an imperfection and must occur generically for all flux-corrected cases. The cold branch of steady solutions is governed by mechanisms similar to the fully coupled case. The warm branch, however, is spurious and disappears. The dynamics of this and consequences for coupled models are discussed. Multiple steady states can be ruled out as a mechanism for El Niño in favor of oscillatory mechanisms. The important role that coupled feedbacks are suggested to play in establishing tropical climatology is referred to as "the climatological version of the Bjerknes hypothesis."

1. Introduction

The El Niño–Southern Oscillation (ENSO) phenomenon is now widely understood to arise by ocean–atmosphere interaction in the tropical Pacific, a paradigm often referred to as the Bjerknes hypothesis. A modern restatement of Bjerknes's (1969) postulate is that ENSO arises as a self-sustained cycle in which anomalies of sea surface temperature (SST) cause the trade winds to strengthen and slacken and that this in turn drives the changes in ocean circulation that produce anomalous SST, with the "memory" for this coupled cycle residing in the ocean. In qualitative terms, one can argue for extending a version of Bjerknes hypothesis to the tropical Pacific climatology itself. As Bjerknes noted, "It seems reasonable to assume that it is the gradient of sea surface temperature along the equator which is the cause of . . . the Walker circulation." The easterly trade winds along the equator in turn maintain the east–west thermocline slope and the equatorial upwelling that together produce the SST gradient between the western Pacific warm pool and the equatorial cold tongue of the eastern Pacific.

Indications of likely involvement of coupled processes in the annual cycle have further been suggested from the relation of seasonal SST, wind fields, and convergence zones (e.g., Philander and Chao 1991; Mitchell and Wallace 1992). However, a clear statement of a "climatological version of the Bjerknes hypothesis" seems to be lacking in the literature. We phrase the conjecture as follows:

> The climatological warm-pool–cold-tongue configuration in the Pacific basin results substantially from ocean–atmosphere feedbacks within the basin. It is useful to distinguish between the atmospheric circulation (especially wind stress) forced "externally" by factors outside the basin and wind stress that is associated with SST gradients within the basin and, thus, with internal coupled feedbacks. While externally forced stress may create longitudinal SST gradients, internal coupled feedbacks significantly enhance these. The spatial form of the warm-pool–cold-tongue pattern depends on the nature of the coupled feedbacks.

Corresponding author address: J. David Neelin, Department of Atmospheric Sciences, University of California at Los Angeles, Los Angeles, CA 90024-1565.
E-mail: neelin@atmos.ucla.edu

Circumstantial evidence that coupled feedbacks within the Pacific basin may be important to the climatology may be inferred from the comparison of tropical simulations of coupled general circulation models (GCMs). These may exhibit climate drift of various forms: the term "drift" is used for both the equilibrium departure of the model climatology from observations and for the process of adjustment toward this equilibrium. In particular, the warm-pool–cold-tongue configuration is not guaranteed to be reproduced in coupled models: the cold tongue can cut right across the basin or migrate to midbasin; the warm pool can be displaced or warm water can occur in the eastern as well as the western basin; weak zonal SST gradients across the equator are common (Neelin et al. 1992; see also Meehl 1990; Gates et al. 1985; Sperber et al. 1987; Gordon 1989; Endoh et al. 1991). Part of such drift can occur on relatively fast timescales characteristic of coupled processes involving dynamical adjustment of the upper ocean. While recent coupled GCMs have shown improvement in tropical simulation (e.g., Philander et al. 1992; Nagai et al. 1992; Gent and Tribbia 1993; Mechoso et al. 1993; Latif et al. 1994), the drift found in earlier attempts or coarser resolution models is instructive in that coupled feedbacks akin to those operating in ENSO can apparently play a significant role in exacerbating errors relative to that of the uncoupled components.

In this series of papers, we attempt to provide a view of the climatological coupled feedbacks in the simplest context that can be considered realistic. The problem of the maintenance of the zonal gradients of SST along the equator is addressed for the *annual average climatology,* neglecting meridional asymmetry between the hemispheres. The "stripped down," intermediate, coupled model of Jin and Neelin (1993a,b) and Neelin and Jin (1993) is employed in combination with continuation techniques (Keller 1977; see, e.g., Ghil and Childress 1987 for atmospheric applications) as in Dijkstra and Neelin (1995a, DN hereafter). This permits direct and efficient solution for stationary states, regardless of stability. Happily, it proves possible to obtain reasonable simulations of the warm-pool–cold-tongue contrast from this approach. In contrast to ENSO, where the timescale has been a focus of attention, the determination of spatial patterns by coupled processes is central to the coupled climatology problem. The relative role of different coupled feedbacks, particularly the upwelling feedback and the thermocline feedback, and their effects on the position and shape of the cold tongue are examined in Part II: a detailed discussion of the factors permitting realistic simulation of the cold tongue is provided therein. Instabilities of this coupled climatology (in the case that includes oscillatory instabilities) are studied in Part III of this series to provide the connection to interannual variability.

Before addressing the details of how coupled feedbacks maintain the climatological state, it proves necessary to first establish whether in fact only a single stationary state is involved. The possibility of multiple stationary states has long provided a red herring in the discussion of ENSO (see section 5 for a brief review), in part because multiple equilibria can indeed occur in ENSO models. The fact that such structures can be generated under some conditions does speak for the potential importance of coupled feedbacks to stationary solutions; however, it is essential to contrast the behavior of the flux-corrected case with that of the fully coupled problem. Here in Part I, we show how these alternate equilibria arise artificially due to "flux correction," where we adopt this term (Sausen et al. 1988) to refer to any of several methods used to construct climatological solutions in coupled models [see, e.g., Manabe and Stouffer (1988) and Zebiak and Cane (1987); the terms "flux adjustment" or "anomaly modeling" are essentially equivalent].

Because sensitivity to the balance of various coupled processes makes satisfactory simulation of the coupled climatology a challenging problem, modelers interested primarily in departures from current climatology often use flux correction to construct the desired climatology. This is eschewed in the current generation of coupled GCMs designed for the tropical problem but used in many global coupled GCMs; it is widespread in simple, intermediate, and hybrid coupled models where the model components are often much less accurate for climate simulation purposes than for simulation of anomalies. A correction is introduced to keep the model near climatology, or a climatological solution is created such that zero anomaly is a solution of the model equations. To make this more precise, let $\bar{T}_{oc}$ indicate the steady or time-average SST field for the uncoupled ocean model forced by observed winds $\bar{\tau}_{obs}$ and let $\bar{T}_{obs}$ indicate the observed time-average SST field. In a two-way flux correction (for atmospheric models A that simulate total winds), the coupling (with flux correction) is established in the following way: the temperature $T^{\uparrow}$ fed into the atmosphere model is given by

$$T^{\uparrow} = \bar{T}_{obs} + T - \bar{T}_{oc}, \tag{1a}$$

where T is the SST of the ocean component of the coupled system. The stress $\tau^{\downarrow}$ fed into the ocean is given by

$$\tau^{\downarrow} = \bar{\tau}_{obs} + A(T^{\uparrow}) - A(\bar{T}_{obs}). \tag{1b}$$

In a one-way flux correction (for atmosphere models that only simulate the evolution of anomalies), the shear stress fed into the ocean model is

$$\tau^{\downarrow} = \bar{\tau}_{obs} + A(T) - A(\bar{T}_{oc}). \tag{1c}$$

In either case, a zero anomaly solution (with $T = \bar{T}_{oc}$) is always a solution of the coupled system; these and other variants of flux correction are equivalent in terms of producing such constructed solutions. Interesting

dynamical behavior is observed through instabilities of this flux-corrected climatology. These instabilities may lead to time-dependent behavior, but if purely growing instabilities occur, they lead (for most physically relevant cases) to a multiplicity of steady states, some of which may be very different from the constructed state and thus climatically unrealistic. Dijkstra and Neelin (1995a) investigated these multiple stationary states in an intermediate model and found complicated structures for the stationary solutions and their interaction with oscillatory solutions. Even in regions of parameter space where all of the stationary states were unstable and thus could not have been directly identified from a time-integrated model, their presence could influence the time-dependent flow.

The stationary branches of flux-corrected models, however, share a common feature: they must arise by transcritical bifurcations (generically) or pitchfork bifurcations (in special cases). Elementary considerations from imperfection theory (e.g., Iooss and Joseph 1990) imply that there must be a topological change in the bifurcation structure as soon as the flux-correction condition is relaxed. In many dynamical systems, such imperfections need not imply drastic changes in the physics of the system, but a combination of physical intuition and generic considerations of how the stationary states must behave suggested to us that for the flux-corrected tropical system, the change would be dramatic.

It is this difference in the structure of stationary solutions, and the physical explanation for it, that we address in this paper. Using the same model as in DN, we study the change in bifurcation structure as the underlying vector field is continuously deformed from the flux-corrected case to the coupled climatology case. The change between the flux-corrected case and the fully coupled case indeed proves fundamental; in the latter, a unique stationary solution remains, which depends nonlinearly on the parameters. This is presented in section 3, and the physical explanation of this topological change in attractor structure is discussed. In section 4, a simple "toy" (point coupling) model is discussed (detailed analysis in the appendix) that proves to be a handy tool to understand the dynamics of the coupled system. The results from the toy model mimic the response computed with the spatially dependent model and neatly illustrate the physics supporting the coupled climatology in the fully coupled case and the reasons for the multiple branches in the flux-corrected case. Section 5 discusses the connection to ENSO literature and possible implications for flux correction in general.

2. Model

The coupled equatorial ocean–atmosphere model used in this study is similar to that presented in DN, Jin and Neelin (1993a), and Neelin and Jin (1993). It is an intermediate model in which an ocean model, consisting of a modified shallow water layer of mean depth H with an embedded mixed layer of fixed depth H_1 is coupled to a Gill-type atmosphere model. In Parts I and II of this paper, we are concerned with stationary solutions of the model and, thus, can make use of the fast wave limit version (Hao et al. 1993; DN) in which the shallow-water component of the model is assumed to adjust quickly compared with the timescales of coupled dynamics. The steady states are the same as for the full system and the solutions are easier to obtain. The linear stability of the steady solutions is only considered with respect to a restricted class of perturbations (i.e., those in the fast wave limit), but only stationary branches are sought. The problem of linear stability to the most general class of perturbations in the model, including time dependence of the shallow-water component, will be the subject of Part III.

We keep the notation as in DN unless specified; in nondimensional variables the SST equation (neglecting zonal advection of SST) is

$$\partial_t T = -\mathscr{H}(w_1)w_1(T - T_s) + \mathscr{H}(-v_N)v_N(T - T_N) - \epsilon_T(T - T_0). \quad (2a)$$

In this equation, $\mathscr{H}(w)$ is a continuous approximation to the Heaviside function, w_1 is the vertical velocity, and v_N is an off-equatorial meridional velocity. The temperature T_0 is the equilibrium SST in absence of any dynamics (i.e., surface heat-flux equilibrium), ϵ_T represents thermal damping rate by surface fluxes, T_N is off-equatorial SST, taken equal to T_0, and T_s is the subsurface temperature. Since only steady states are considered, the ocean is in Sverdrup balance. In the limit of negligible oceanic damping, the vertical velocity contributed by the shallow-water component is zero and the thermocline is given by (Hao et al. 1993)

$$h(x) = \int_0^1 s^{1/2}\tau(s)ds - \int_x^1 \tau(s)ds, \quad (2b)$$

where $\tau(s)$ is the equatorial zonal wind stress. The velocities w_1 and v_N are created by Ekman dynamics and given by

$$w_1 = -\delta_s\tau; \quad -v_N = \delta_s\tau, \quad (2c)$$

where the surface-layer parameter δ_s depends inversely on the mixing rate between the surface layer and the remainder of the layer above the thermocline. We note that zonal advection is neglected in SST and surface currents because it does not qualitatively change the results. However, zonal mass transport in the thermocline layer *is* included in the derivation of (2b).

The subsurface temperature T_s depends on h according to

$$T_s(h) = T_{s0} + (T_0 - T_{s0})\tanh(\eta_1 h + \eta_2), \quad (2d)$$

with $\eta_1 = H/H_*$, $\eta_2 = h_0/H_*$, and where h_0 and H_* control the steepness and the offset of the T_s profile.

TABLE 1. Standard values of parameters in the intermediate model. Nondimensionalization as in DN.

$T_0 = 30$	$T_N = 30$	$T_{s0} = 24$
$\eta_1 = 6.667$	$\eta_2 = 0.833$	$\delta_F = 4.104$
$\epsilon_T = 0.694$	$\epsilon_a = 2.5$	

The reference value of the subsurface temperature T_{s0} is quantitatively important since $(T_0 - T_{s0})$ sets a scale for SST anomalies but is qualitatively unimportant because solutions for different T_{s0} are related by a simple rescaling.

In a one-way flux correction, the ocean is forced with the observed mean wind stress $\bar{\tau}_{\text{obs}}$, the resulting steady-state temperature being $\bar{T}$. In coupling the system, the surface shear stress τ fed into the ocean model then becomes

$$\tau = \bar{\tau}_{\text{obs}} + \mu(A(T) - A(\bar{T})), \tag{3}$$

where A is the particular atmosphere model used and μ is the coupling parameter. Hence, there is a constructed solution $T = \bar{T}$, $\tau = \bar{\tau}_{\text{obs}}$ (referred to as the flux-corrected climatology) that does not depend on coupling. The latter affects only the stability of this state to perturbations. When a simple linear Gill atmosphere model is used, the operator A is given by

$$A(T) = 2\exp(3\epsilon_a x)\int_x^1 \exp(-3\epsilon_a s)T(s)ds - \frac{2}{3}\exp(-\epsilon_a x)\int_0^x \exp(\epsilon_a s)T(s)ds, \tag{4}$$

where ϵ_a is the dimensionless atmospheric damping length. It is known (DN; Hao et al. 1993) that the state $\bar{T}$ undergoes either transcritical or Hopf bifurcations as μ is increased. Standard values of oceanic and atmospheric model parameters are given in Table 1. A value of $\delta_s = 1.0$ is used throughout this part; for consistency with DN a fixed value of this surface layer parameter, denoted δ_F, is used in establishing the flux-corrected ocean climatology.

For models that attempt to simulate the full tropical coupled ocean–atmosphere system, the determination of the climatology is a major end in itself. This climatology depends on coupling strength and the value of other parameters in the model. For the case of a model with active ocean only in a single basin (here the Pacific), there will be a part of the wind stress that depends on the atmospheric response to the temperature pattern within the basin and a part, $\bar{\tau}_{\text{ext}}$, that is determined externally. The part determined within the basin will depend on temperature departures $T - T_0$ from surface heat flux equilibrium; thus,

$$\tau = \bar{\tau}_{\text{ext}} + \mu A(T - T_0), \tag{5a}$$

where $T - T_0 = 0$ is assumed outside the basin (as appropriate for continental conditions). For the external part $\bar{\tau}_{\text{ext}}$, we consider a zonally constant component, for example, due to the zonally symmetric circulation. Since the latter obeys strong dynamical constraints, it will depend relatively little on the coupled dynamics within the basin compared with the Walker-type circulation $A(T - T_0)$ driven by zonal gradients. A more extensive discussion of the form of $\bar{\tau}_{\text{ext}}$ and T_0 is given in Part II (Dijkstra and Neelin 1995b). The stationary state is easily computed at $\mu = 0$ but depends on coupled feedbacks otherwise. This provides a close analog to the problem faced by coupled GCMs in terms of a number of three-dimensional dynamical feedbacks. We refer to Eq. (5a) as the "coupled climatology" case.

In this paper we ask how the bifurcation structure of the flux-corrected case changes as we relax the restriction of flux correction toward the more difficult coupled climatology case. To this end, we split the observed wind stress into the part $\bar{\tau}_{\text{ext}}$ [considered to originate from processes outside the basin, chosen zonally constant as in (5a)] and the remainder $\bar{\tau}_{\text{obs}} - \bar{\tau}_{\text{ext}}$. To be able to follow the deformation of the bifurcation diagram, we introduce a homotopy parameter α_F. The shear stress τ is then given by

$$\tau = \bar{\tau}_{\text{ext}} + \alpha_F(\bar{\tau}_{\text{obs}} - \bar{\tau}_{\text{ext}}) + \mu\{\alpha_F A(T - \bar{T}) + (1 - \alpha_F)A(T - T_0)\}, \tag{5b}$$

where $\bar{T}$ still refers to the (constructed) equilibrium state with $\tau = \bar{\tau}_{\text{obs}}$. It is clear that for $\alpha_F = 1$, the flux-corrected problem is recovered. For $\alpha_F = 0$, there is no flux correction and we obtain the coupled climatology case. Equilibrium solutions will be determined by the zonally constant shear stress of magnitude $\bar{\tau}_{\text{ext}}$ and the full feedback processes within the basin. The path that is taken between both extreme cases is sketched in Fig. 1.

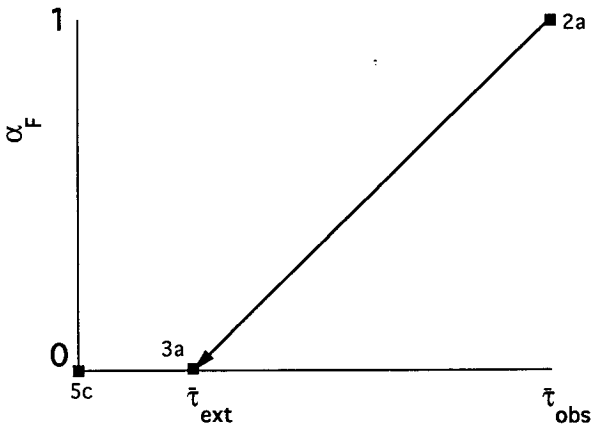

FIG. 1. Path in parameter space between the flux-corrected case and the fully coupled case. The abscissa α_F is the parameter that governs this transition; the ordinate is a measure of the strength of the (easterly) wind stress over the basin. A second path segment (3a–5c) is used to examine the effect of $\bar{\tau}_{\text{ext}}$ within the fully coupled case ($\alpha_F = 0$). The labels refer to subsequent figures that contain bifurcation diagrams at the locations indicated.

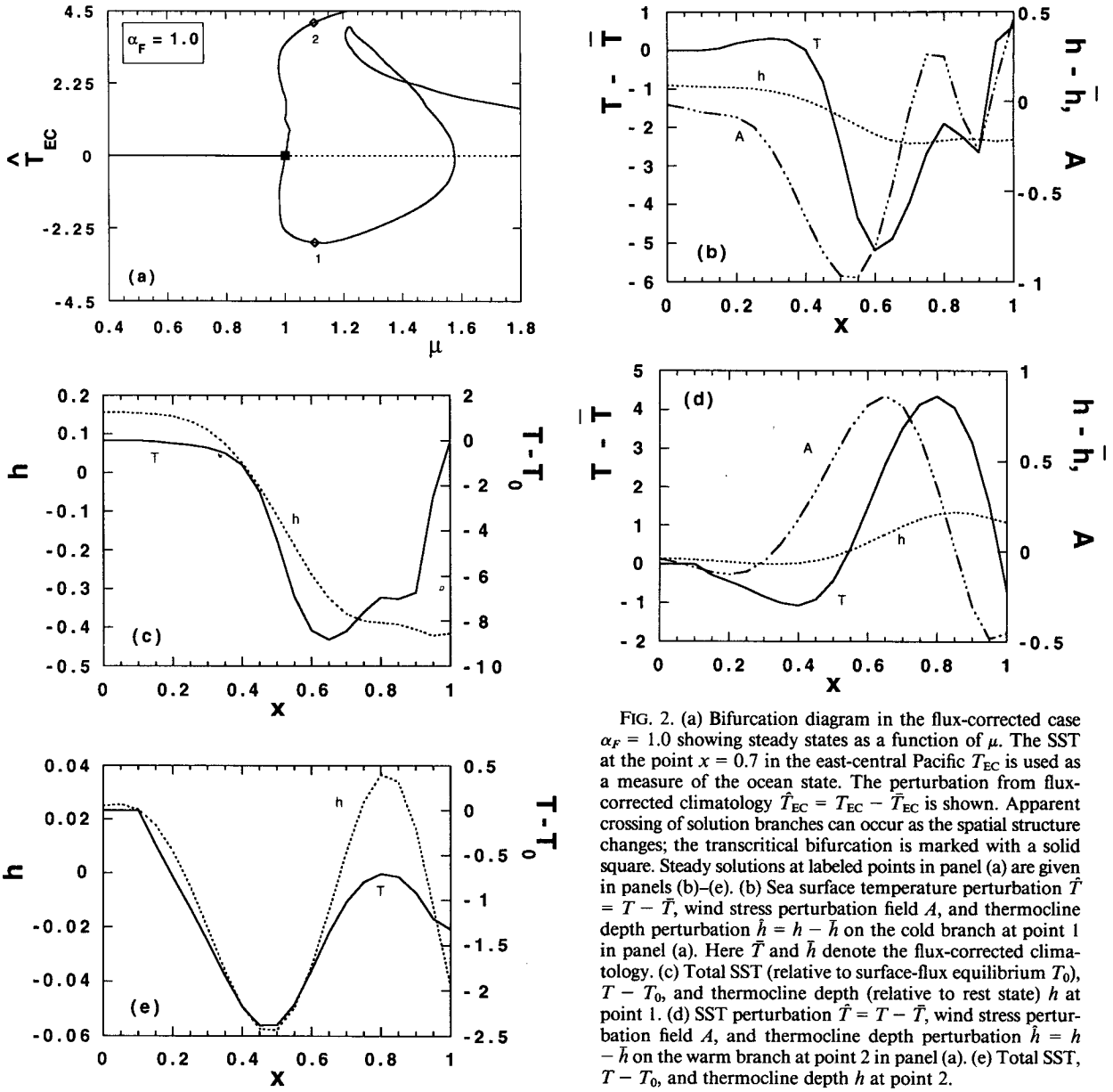

FIG. 2. (a) Bifurcation diagram in the flux-corrected case $\alpha_F = 1.0$ showing steady states as a function of μ. The SST at the point $x = 0.7$ in the east-central Pacific T_{EC} is used as a measure of the ocean state. The perturbation from flux-corrected climatology $\hat{T}_{EC} = T_{EC} - \bar{T}_{EC}$ is shown. Apparent crossing of solution branches can occur as the spatial structure changes; the transcritical bifurcation is marked with a solid square. Steady solutions at labeled points in panel (a) are given in panels (b)–(e). (b) Sea surface temperature perturbation $\hat{T} = T - \bar{T}$, wind stress perturbation field A, and thermocline depth perturbation $\hat{h} = h - \bar{h}$ on the cold branch at point 1 in panel (a). Here $\bar{T}$ and $\bar{h}$ denote the flux-corrected climatology. (c) Total SST (relative to surface-flux equilibrium T_0), $T - T_0$, and thermocline depth (relative to rest state) h at point 1. (d) SST perturbation $\hat{T} = T - \bar{T}$, wind stress perturbation field A, and thermocline depth perturbation $\hat{h} = h - \bar{h}$ on the warm branch at point 2 in panel (a). (e) Total SST, $T - T_0$, and thermocline depth h at point 2.

To distinguish coupled from uncoupled contributions to the solution in the fully coupled case, it is convenient to define T_{ext} and h_{ext} to be the response of the uncoupled ocean to the external wind stress $\bar{\tau}_{ext}$. Then the contribution associated with coupling is $\hat{T} = T - T_{ext}$, etc. In the flux-corrected case, the corresponding quantity is $\hat{T} = T - \bar{T}$ with $\bar{T}$ the constructed climatology. To include the cases in between, we simply define $\hat{T} = T - T(\mu = 0)$ for $0 \leq \alpha_F \leq 1$.

3. Results

a. *Transition from the flux-corrected climatology to the coupled climatology*

We first consider the case $\bar{\tau}_{ext} = -0.2$ and

$$\bar{\tau}_{obs} = 0.6\{0.12 - \cos^2[(x - x_0)\pi/(2x_0)]\}, \quad x_0 = 0.57. \quad (6)$$

This wind field is the same as used in Hao et al. (1993) and DN and corresponds roughly to observed mean equatorial winds. The bifurcation picture for $\alpha_F = 1.0$ (Fig. 2a) corresponds to Fig. 8a in DN. The flux-corrected state becomes unstable at a transcritical bifurcation near $\mu = 1.0$. From this singularity, two new branches of steady states appear. On each branch, solutions at labeled points are shown in the Figs. 2b–e. Solutions on the lower branch have a relatively cold eastern basin (Figs. 2b–c). On the upper branch, there is a relatively warm eastern basin (Figs. 2d–e). In strong

contrast to Fig. 2a, in the bifurcation diagram for the coupled climatology case ($\alpha_F = 0$, Fig. 3a), no bifurcations occur and there is only one solution over the range of μ considered. The spatial patterns of perturbation and total fields are given in Figs. 3b,c at a labeled point in Fig. 3a ($\mu = 1.1$). These structures closely resemble those of the flux-corrected case on the "cold" branch (Figs. 2b–c).

How can the connection occur between the bifurcation diagrams in the Figs. 2a and 3a? What happens to the "warm" branch present in Fig. 2a? The answer is obtained from Fig. 4a where bifurcation diagrams for intermediate α_F are given. These pictures have no direct physical significance individually, but show clearly the transition in parameter space between the physically relevant cases $\alpha_F = 0$ and $\alpha_F = 1$. When α_F is decreased slightly to $\alpha_F = 0.99$, the transcritical bifurcation is broken. However, the spatial structure of the solutions for $\alpha_F = 0.99$ at $\mu = 1.1$ remain nearly identical to those in Figs. 2b–e. With decreasing α_F, the upper branch quickly moves to larger μ (see the branch for $\alpha_F = 0.95$), indicating that the states on this branch (see Figs. 4b,c at labeled point 1 in Fig. 4a) can only be maintained through large coupling. The warm anomalies in the eastern Pacific seen in Fig. 2d have been considerably reduced in Fig. 4c despite an increase in μ (1.65 in Fig. 4c vs 1.1 in Fig. 2d), associated with the relaxation of flux correction. The "cold" branch, however, hardly changes with decreasing α_F (Fig. 4a, $\alpha_F = 0.95$). This indicates that for this state, the upwelling and thermocline slope that were maintained by prescribed winds in the flux-corrected case can still be maintained by coupled processes. With decreasing α_F only this branch remains and is deformed smoothly into the coupled climatology branch of Fig. 3a.

To understand this behavior qualitatively, especially the shift of the warm branch to larger values of coupling, we rewrite equation (5b) as

$$\tau = [\bar{\tau}_{\text{ext}} + \alpha_F(\bar{\tau}_{\text{obs}} - \bar{\tau}_{\text{ext}})] + \mu\{A(T - T_0) + \alpha_F A(T_0 - \bar{T})\}. \quad (5b')$$

The term between the square brackets represents a large-scale easterly wind of which the magnitude does not vary much if α_F is close to 1 and remains easterly, though smaller, as $\alpha_F \to 0$. Of the terms that multiply μ, the second term $A(T_0 - \bar{T})$ corresponds to large-scale westerlies. These westerlies, which are introduced by flux correction, are essential in maintaining the warm branch, which has a relatively warm eastern basin. Their structure is fixed by the flux-corrected climatology and hence only the magnitude can be changed by coupling. On the contrary, the first term multiplying μ represents coupled easterly winds, which can change according to a temperature variation. If α_F is decreased, the solution on the warm branch can only be maintained if μ increases to

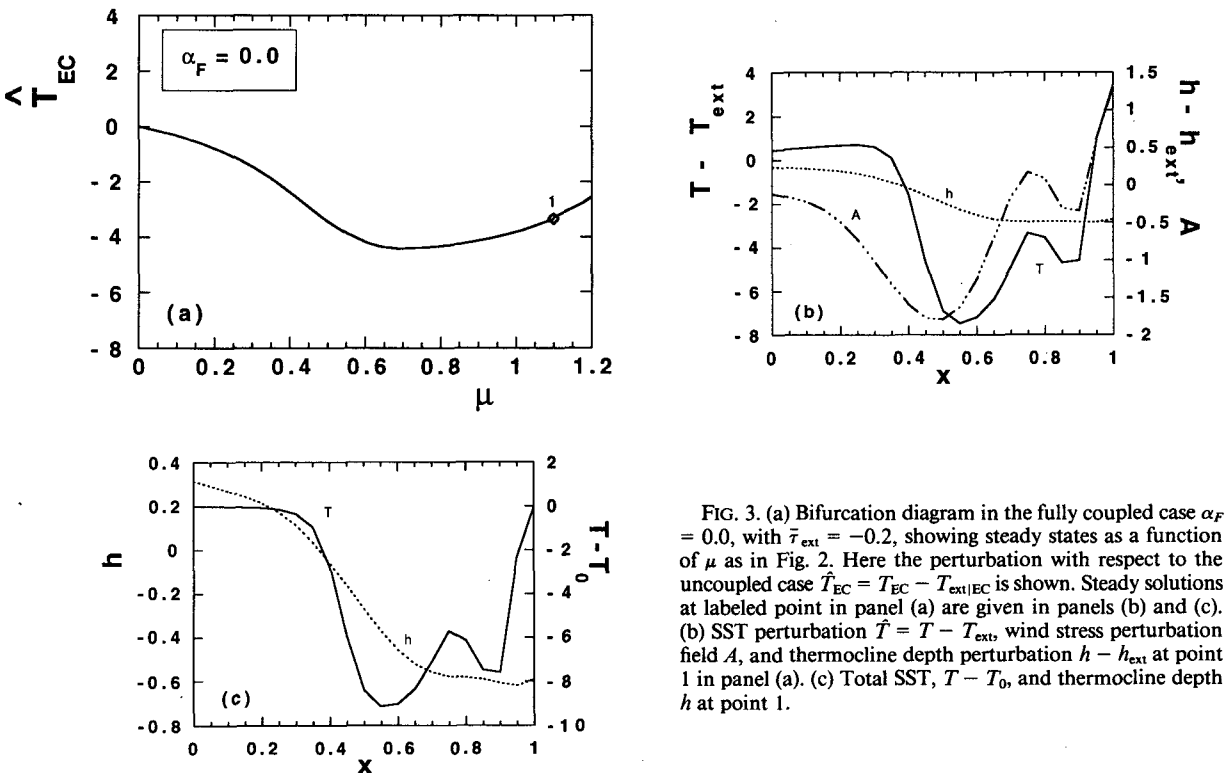

FIG. 3. (a) Bifurcation diagram in the fully coupled case $\alpha_F = 0.0$, with $\bar{\tau}_{\text{ext}} = -0.2$, showing steady states as a function of μ as in Fig. 2. Here the perturbation with respect to the uncoupled case $\hat{T}_{\text{EC}} = T_{\text{EC}} - T_{\text{ext|EC}}$ is shown. Steady solutions at labeled point in panel (a) are given in panels (b) and (c). (b) SST perturbation $\hat{T} = T - T_{\text{ext}}$, wind stress perturbation field A, and thermocline depth perturbation $h - h_{\text{ext}}$ at point 1 in panel (a). (c) Total SST, $T - T_0$, and thermocline depth h at point 1.

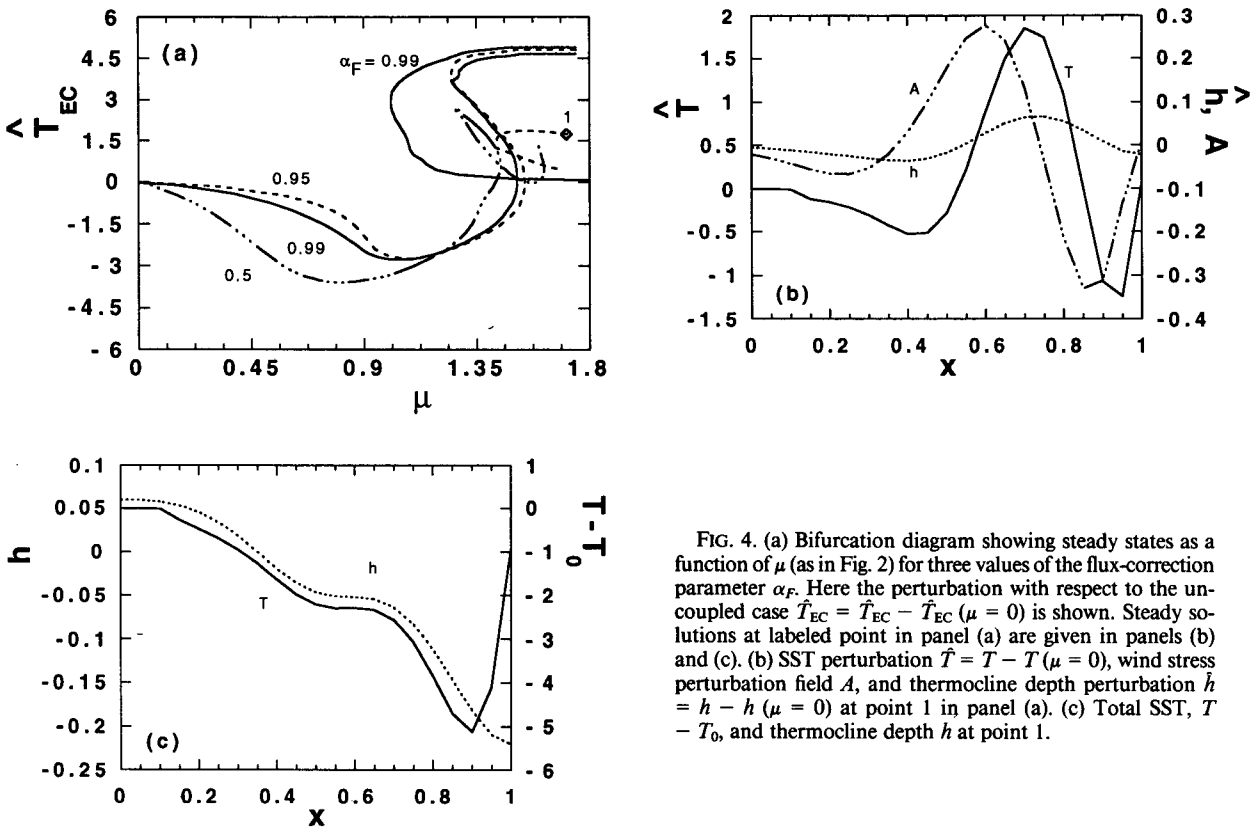

FIG. 4. (a) Bifurcation diagram showing steady states as a function of μ (as in Fig. 2) for three values of the flux-correction parameter α_F. Here the perturbation with respect to the uncoupled case $\hat{T}_{EC} = \hat{T}_{EC} - \hat{T}_{EC}$ ($\mu = 0$) is shown. Steady solutions at labeled point in panel (a) are given in panels (b) and (c). (b) SST perturbation $\hat{T} = T - T$ ($\mu = 0$), wind stress perturbation field A, and thermocline depth perturbation $\hat{h} = h - h$ ($\mu = 0$) at point 1 in panel (a). (c) Total SST, $T - T_0$, and thermocline depth h at point 1.

maintain the contribution of the westerlies essential to the balances on this branch. Eventually, the warm branch will disappear by moving to infinite μ in the limit $\alpha_F \to 0$. On the cold branch, in contrast, the coupled system is able to produce easterlies by internal feedbacks as the flux correction is relaxed. This is possible because the temperature difference $(T - T_0)$ in the $\mu A(T - T_0)$ term can be self-consistently maintained at finite negative values by a combination of upwelling and thermocline feedbacks. The temperature can thus adjust at fixed μ to a change in α_F to maintain the balances on the branch while the artificial westerly wind contribution vanishes (as $\alpha_F \to 0$).

b. *Influence of external wind*

When $\bar{\tau}_{ext}$ is small (-0.01), the bifurcation structures change with α_F as shown in Fig. 5a. For α_F near unity, the same transition structure is found, since this hardly depends on $\bar{\tau}_{ext}$ as long as this quantity is significantly smaller than the maximum amplitude of $\bar{\tau}_{obs}$. At $\alpha_F = 0.5$ and $\mu = 1.1$ (point 1 in Fig. 5b), smaller-scale internal structure is found within the cold tongue (Figs. 6a,b) (i.e., two SST minima occur within the cold tongue). When α_F is further decreased, first the branch winds around and for a value slightly larger than $\alpha_F = 0.2$, the loop is pinched off, forming an isola and a simple stable (for the range of μ shown) branch. The isola shrinks to one point at $\alpha_F \approx 0.11$ and the simple branch remains. At this branch (point 2 in Fig. 5b), the smaller-scale structure within the cold tongue has disappeared and a smooth temperature profile (Figs. 6c,d) with a cold tongue in the center of the basin remains.

The final bifurcation picture at the coupled climatology case $\alpha_F = 0.0$ is shown in Fig. 5c. The amplitudes of the temperature perturbations remain small even at large coupling. This indicates that the externally forced wind stress $\bar{\tau}_{ext}$ is important in setting the amplitude of a reasonable coupled tropical climatology. The steady state at $\mu = 1.1$ (Figs. 7a,b at point 1 in Fig. 5c) is an unrealistic coupled climatology with a cold tongue in the west and a warm pool in the east. Although this climatology is almost completely (up to the part due to $\bar{\tau}_{ext}$) determined by coupled processes in the basin, the parameters are such that upwelling is not strong enough in the eastern part of the basin. An increase of coupling strength makes the situation even worse (point 2, $\mu \approx 2.6$, Figs. 7c,d). Of course, it might be possible to change the other parameters in such a way as to obtain a good climatology; this is indeed the case, as shown in Part II of this paper. The main point of the results above is that the structure of the steady states

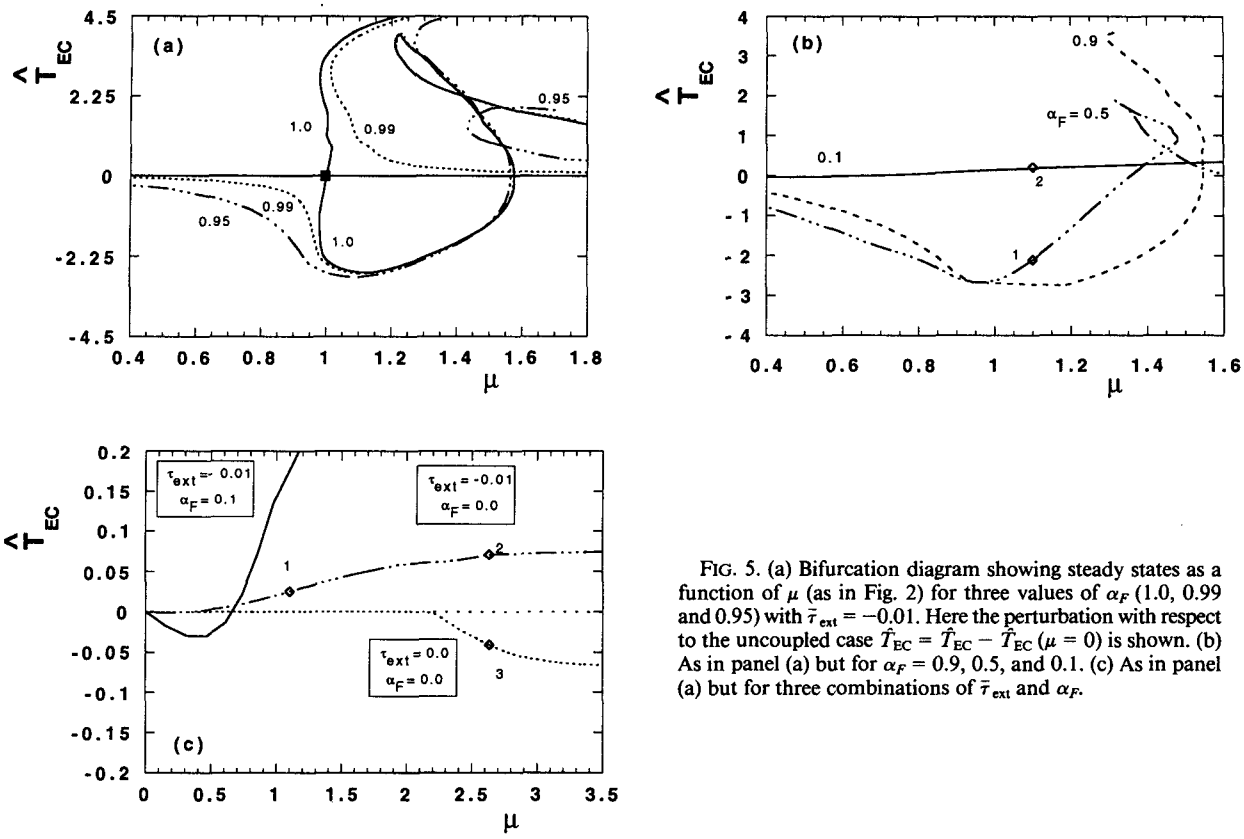

FIG. 5. (a) Bifurcation diagram showing steady states as a function of μ (as in Fig. 2) for three values of α_F (1.0, 0.99 and 0.95) with $\bar{\tau}_{ext} = -0.01$. Here the perturbation with respect to the uncoupled case $\hat{T}_{EC} = \hat{T}_{EC} - \hat{T}_{EC}$ ($\mu = 0$) is shown. (b) As in panel (a) but for $\alpha_F = 0.9$, 0.5, and 0.1. (c) As in panel (a) but for three combinations of $\bar{\tau}_{ext}$ and α_F.

differs substantially for the flux-corrected case, where there are multiple equilibria, compared with the coupled climatology case where the climate state might or might not be realistic, but is generally unique.

One might ask what structure remains (and if any multiplicity of solutions occurs) at large coupling when $\bar{\tau}_{ext}$ is decreased to zero; this bifurcation diagram is also shown in Fig. 5c. The trivial state (which corresponds to a constant overall temperature) is in this limit a solution of the coupled climatology case: at large values of μ, however, another (nontrivial) solution exists, arising by a bifurcation at $\mu \approx 2.2$ in Fig. 5c. Symmetry breaking from the trivial state and multiplicity of solutions may therefore occur at large coupling due to coupled processes within the basin even without any external forcing. We emphasize that this is a special case, which is useful for its conceptual value, rather than a case that could occur in a coupled GCM. The trivial state at large μ disappears if any of several perturbations to the model vector field are introduced, for instance, a tiny value of $\bar{\tau}_{ext}$ or adding a small entrainment velocity to the ocean model. The model then reverts to a single stationary state with the form of the branch as shown in Fig. 5c. We address this symmetry breaking in more detail and show how it arises in a simple "toy" model below. The spatial pattern on the nontrivial cold branch that arises from the symmetry breaking (point 3, $\mu \approx 2.6$, Figs. 7e, f) is quite "wiggly" with a sharp cold tongue between warm regions in the central and eastern part of the basin.

4. A "toy" model

a. *Formulation of the model*

The breakup of the transcritical bifurcation through an imperfection as well as the symmetry breaking observed in Fig. 5c may be understood more clearly by considering a "toy" model in which the atmospheric wind response to SST is purely local:

$$A(T') = \mu A_0 T', \tag{7a}$$

where A_0 is a scalar and T' is the perturbation from the appropriate reference temperature. In the flux-corrected case $T' = \hat{T} = T - \bar{T}$ (where $\hat{T}$ is consistent with our previous usage); in the fully coupled case $T' = T - T_0$ (which differs from $\hat{T} = T - T_{ext}$). Choosing $A_0 > 0$ for westerlies over warm SST, we can absorb A_0 into μ (or simply put $A_0 = 1$). Similarly, thermocline depth is parameterized to deepen locally under a westerly wind stress τ and the surface layer velocities are given by

$$h = \tau; \quad w = -\delta_s \tau; \quad -v_N = \delta_s \tau \tag{7b}$$

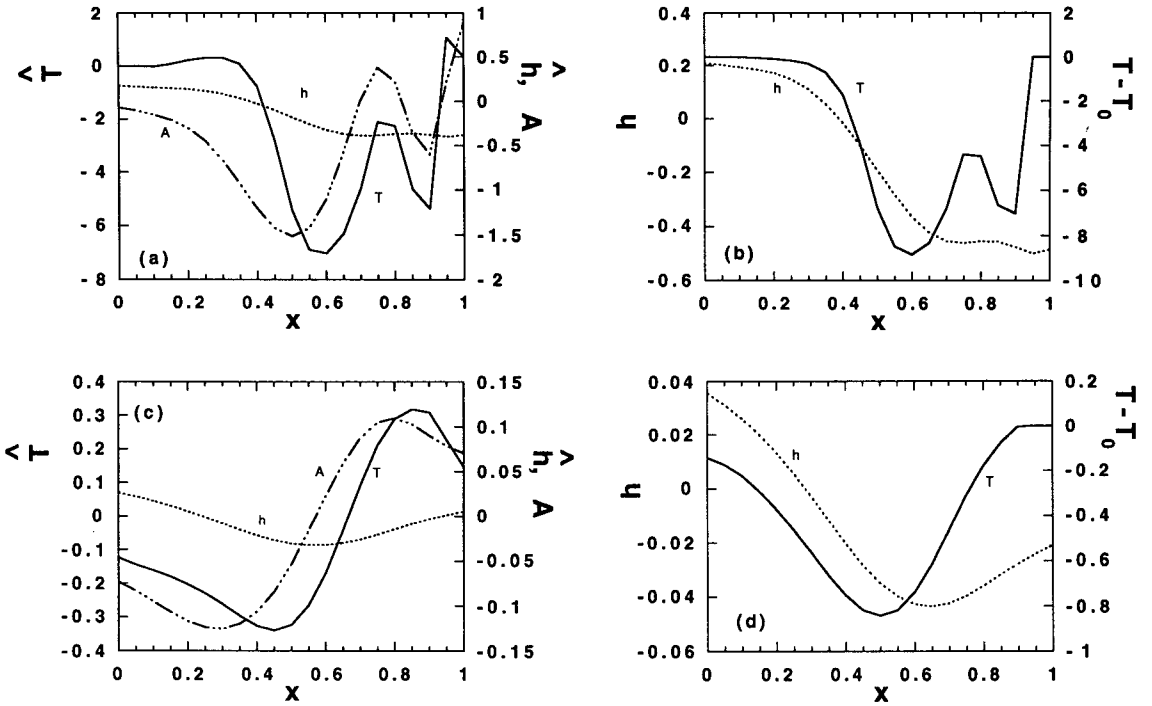

FIG. 6. Steady solutions at labeled points in Fig. 5b. (a) SST perturbation $\hat{T} = T - \bar{T}(\mu = 0)$, wind stress perturbation field A, and thermocline depth perturbation $\hat{h} = h - \bar{h}(\mu = 0)$ at point 1. (b) Total SST, $T - T_0$, and thermocline depth h at point 1. (c) SST perturbation $\hat{T} = T - \bar{T}(\mu = 0)$, wind stress perturbation field A, and thermocline depth perturbation $\hat{h} = h - \bar{h}(\mu = 0)$ at point 2. (d) Total SST, $T - T_0$, and thermocline depth h at point 2.

with the scale of h suitably chosen. The SST equation has the same form as (2a) but for T now being a scalar variable. As in the spatially dependent model, we introduce a homotopy parameter α_F and write the total wind stress τ as

$$\tau = \bar{\tau}_{\text{ext}} + \alpha_F(\bar{\tau}_{\text{obs}} - \bar{\tau}_{\text{ext}}) + \mu[\alpha_F(T - \bar{T}) + (1 - \alpha_F)(T - T_0)], \quad (8)$$

where $\bar{T}$ is the flux-corrected solution for $\alpha_F = 1$ (the response to "observed" wind stress $\bar{\tau}_{\text{obs}}$). Furthermore, T_0 is the surface heat flux equilibrium temperature and $\bar{\tau}_{\text{ext}}$ corresponds to the external wind stress. For continuity, we use $\bar{\tau}_{\text{obs}}$ to denote the analog to the observed stress in the full model, although this is just a scalar value with a magnitude typical of observed eastern Pacific easterlies.

While these simplifications are without formal justification, they can mimic the response of a spatially dependent model in cases where the spatial structure tends to give in-phase relations among stress, $\hat{T}$, and h; for instance, in Hao et al. (1993) this model was used with some success to discuss the qualitative behavior of the stationary bifurcations for the flux-corrected problem. The form of the nonlinearity in the SST equation closely follows that of the intermediate model and differs in important aspects from the simple forms assigned in other toy models (Suarez and Schopf 1988; Battisti and Hirst 1989; Münnich et al. 1991); as far as stationary states are concerned, it can be regarded as an extension of these models. We use a piecewise continuous version of the T_s parameterization

$$T_s(h) = T_1, \quad h \geq h_1;$$
$$T_s(h) = T_2, \quad h \leq h_2;$$
$$T_s(h) = T_2 + \gamma(h - h_2), \quad h_1 \geq h \geq h_2; \quad (9)$$

where $\gamma = (T_1 - T_2)/(h_1 - h_2) \geq 0$ and $T_2 \leq T_1 \leq T_0$; $h_1 \leq h_2$. The steady temperature equation, due to the local approximations, reduces to the single scalar equation for T:

$$\mathscr{H}(w)w[T - T_s(h)] - \mathscr{H}(-v_N)v_N(T - T_N) + \epsilon_T(T - T_0) = 0, \quad (10)$$

where $\mathscr{H}$ is the Heaviside function and h, w, and v_N are given by

$$w = w_0 - \mu\delta_s[\alpha_F(T - \bar{T}) + (1 - \alpha_F)(T - T_0)], \quad v_N = w \quad (11a)$$

with

$$w_0 = -\delta_s[\bar{\tau}_{\text{ext}} + \alpha_F(\bar{\tau}_{\text{obs}} - \bar{\tau}_{\text{ext}})] \quad (11b)$$

and

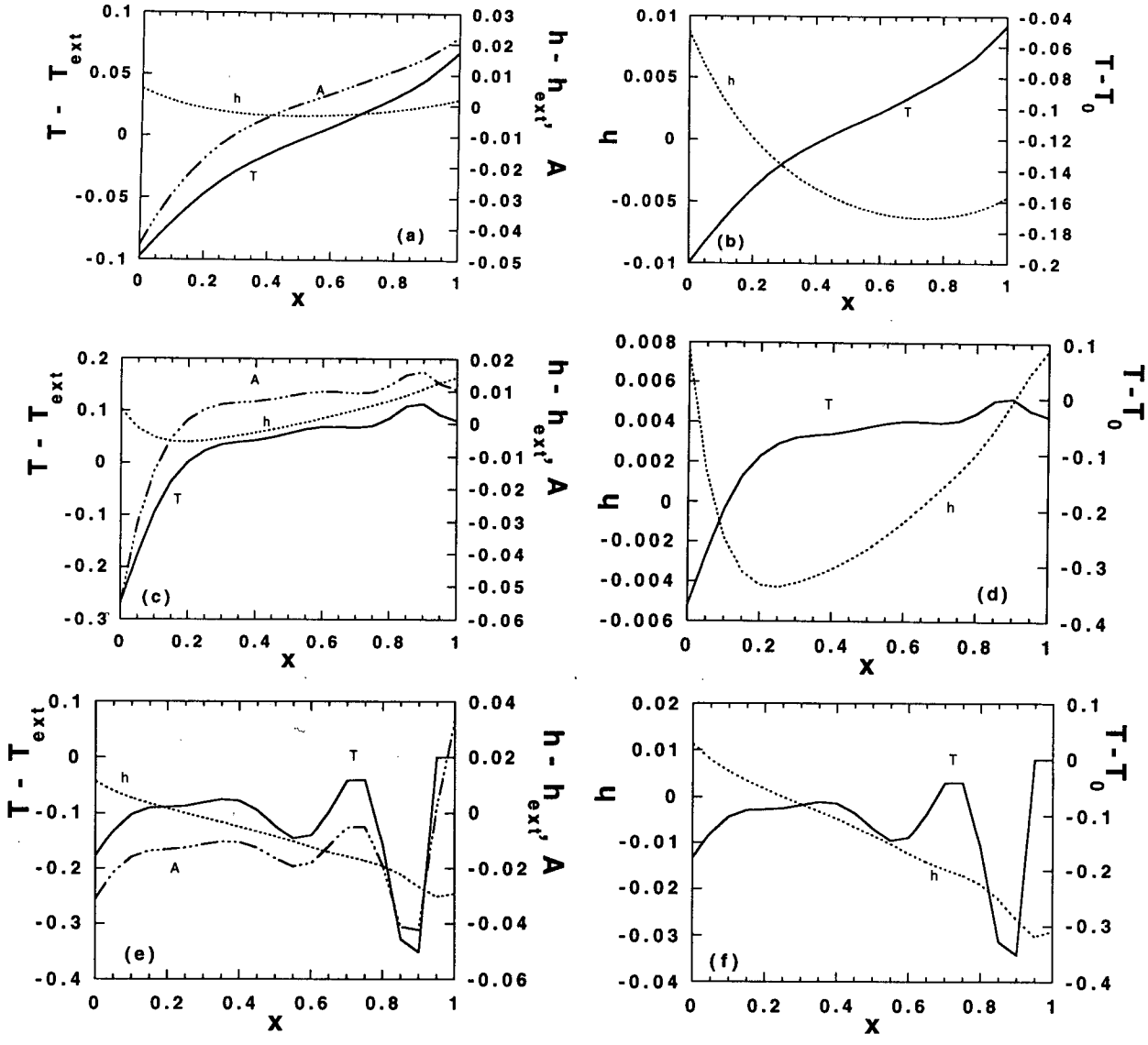

FIG. 7. Steady solutions at labeled points in Fig. 5c. (a) SST perturbation $\hat{T} = T - T_{\text{ext}}$, wind stress perturbation field A, and thermocline depth perturbation $\hat{h} = h - h_{\text{ext}}$ at point 1. (b) Total SST, $T - T_0$, and thermocline depth h at point 1. (c) SST perturbation $\hat{T} = T - T_{\text{ext}}$, wind stress perturbation field A, and thermocline depth perturbation $\hat{h} = h - h_{\text{ext}}$ at point 2. (d) Total SST, $T - T_0$, and thermocline depth h at point 2. (e) SST perturbation $\hat{T} = T - T_{\text{ext}}$, wind stress perturbation field A, and thermocline depth perturbation $\hat{h} = h - h_{\text{ext}}$ at point 3. (f) Total SST, $T - T_0$, and thermocline depth h at point 3.

$$h = \bar{\tau}_{\text{ext}} + \alpha_F(\bar{\tau}_{\text{obs}} - \bar{\tau}_{\text{ext}}) + \mu[\alpha_F(T - \bar{T}) + (1 - \alpha_F)(T - T_0)]. \quad (11c)$$

b. *Analysis of the breaking of the transcritical bifurcation*

Consider first the flux-corrected case $\alpha_F = 1$ with $\delta_s \neq 0$, $\bar{\tau}_{\text{obs}} \leq 0$, $T_N = T_0$ (as we did in the spatially dependent model), and hence $w_0 = -\delta_s \bar{\tau}_{\text{obs}} \geq 0$. As an alternative, we can view w_0 to be independent of $\bar{\tau}_{\text{obs}}$ giving it the interpretation of an entrainment velocity. The flux-corrected solution ($\bar{T}$) is then given by

$$\bar{T} = (\epsilon_T + w_0)^{-1}[w_0 T_{\text{sub}}(\bar{h}) + \epsilon_T T_0] \quad (12a)$$

$$\bar{h} = \bar{\tau}_{\text{obs}}. \quad (12b)$$

By construction, (12) is a solution (the primary branch) for all values of μ. To determine bifurcation points on the primary branch, we search for nearby nontrivial solutions (note that $w > 0$ in a neighborhood of this primary branch). This gives [from (10)]

$$(w_0 - \mu\delta_s\hat{T})[\hat{T} + \bar{T} - T_s(\bar{h} + \mu\hat{T})] + \epsilon_T(\bar{T} + \hat{T} - T_0) = 0, \quad (12c)$$

where $\hat{T} = T - \bar{T}$. Linearization around $\hat{T} = 0$ gives

$$\hat{T}\{w_0(1 - \mu\eta) - \mu\delta_s[\bar{T} - T_s(\bar{h})] + \epsilon_T\} = 0, \quad (13a)$$

where $\eta = dT_s/dh$, evaluated at $h = \bar{h}$. From (9) we see that either $\eta = 0$ or $\eta = \gamma$ depending on the chosen value of $\bar{h}$. Formally, η does not exist at h_1 and h_2, but this is not essential; we could smooth T_s appropriately. Bifurcation occurs at $\mu = \mu_c$ with

$$\mu_c = \{\eta w_0 + \delta_s[\bar{T} - T_s(\bar{h})]\}^{-1}(w_0 + \epsilon_T). \quad (13b)$$

Because $\bar{T} - T_s(\bar{h}) = \epsilon_T[T_0 - T_s(\bar{h})]/(\epsilon_T + w_0) \geq 0$, indeed $\mu_c \geq 0$. To demonstrate that a transcritical bifurcation occurs, note that (12c) can be written as

$$(\mu - \mu_c)\mu_c^{-1}(w_0 + \epsilon_T)\hat{T} + \mu\delta_s(1 - \mu\eta)\hat{T}^2 = 0. \quad (13c)$$

Apart from the trivial solution, there is another solution given by

$$\hat{T} = -(\mu - \mu_c)(w_0 + \epsilon_T)[\mu\mu_c\delta_s(1 - \mu\eta)]^{-1}. \quad (13d)$$

This nontrivial solution crosses the zero solution at an angle, indicating a transcritical bifurcation. If δ_s is not too small, then for small $(\mu - \mu_c)/\mu_c$, the nontrivial solution has the opposite sign as that of $\mu - \mu_c$; for very small δ_s the slope of this nontrivial branch can reverse. The stability of the solution is also determined by the sign of $\mu - \mu_c$: if δ_s is not too small, then for $\mu > \mu_c$, the solution is stable; for $\mu < \mu_c$ the solution is unstable.

For a specific example (values of parameters as in Table 2), this solution structure is shown in Fig. 8a for $\alpha_F = 1.0$. The supercritical branch remains stable. Along the subcritical branch the total vertical velocity becomes smaller, and at the value of μ, where $\mu\delta_s(T - \bar{T}) = w_0$, the upwelling–downwelling nonlinearity is hit. Solutions are then determined [from (10)] by

$$(\epsilon_T + \mu\delta_s\hat{T} - w_0)(\hat{T} + \bar{T} - T_0) = 0. \quad (14)$$

This has only two solutions, $\hat{T} = (w_0 - \epsilon_T)/\mu\delta_s$ and $\hat{T} = T_0 - \bar{T}$. The first coincides with the trivial solution in the specific example shown in Fig. 8a; the other branch is stable and corresponds to the warm (constant) branch in Fig. 8a.

For $\alpha_F \in [0, 1)$ and $w > 0$ we can write (10) as

$$a_1\hat{T}^2 + a_2\hat{T} + a_3 = 0, \quad (15)$$

where the coefficients a_1, a_2, and a_3 can be easily calculated. Notably, a_3 is proportional to $1 - \alpha_F$, so when

TABLE 2. Standard values of parameters for the toy model.

$h_1 = 0.5$	$T_0 = 30$	$T_N = 30$
$h_2 = -0.5$	$T_1 = 30$	$T_2 = 14$
$\delta_s = 1.25$	$\epsilon_T = 1.0$	$\bar{\tau}_{obs} = -0.8$

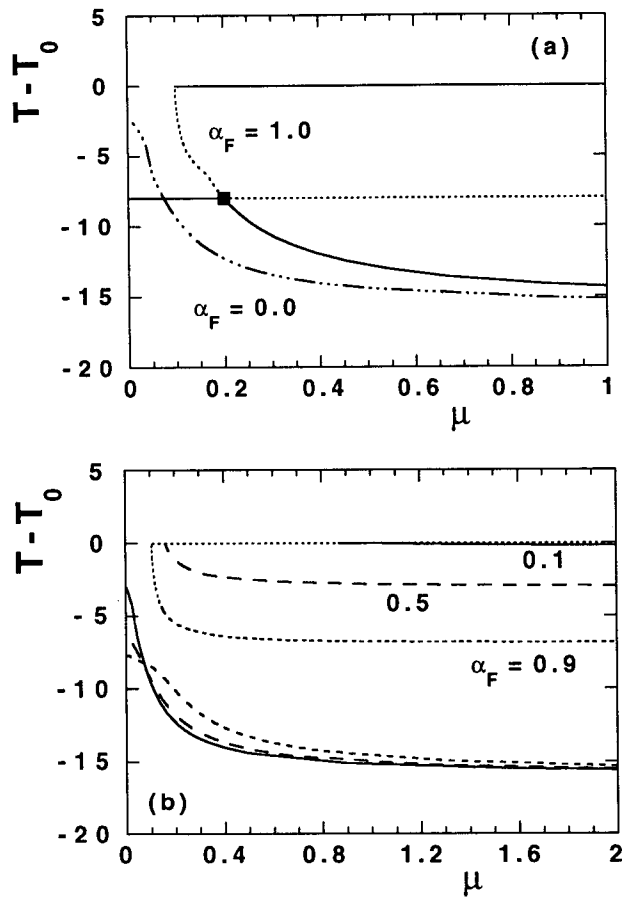

FIG. 8. (a) Bifurcation picture for the "toy" model, both for the flux-corrected case ($\alpha_F = 1.0$) and the fully coupled case ($\alpha_F = 0.0$). The values of the other parameters used are given in Table 2. Flux-corrected case: solid curve where stable, dashed where unstable; transcritical bifurcation marked with a square. Fully coupled case: dash–dot curve. (b) Transition between both curves in Fig. 8a shown by plotting bifurcation structures for several values of α_F. Short dashed lines $\alpha_F = 0.9$; long dashed lines $\alpha_F = 0.5$; solid lines $\alpha_F = 0.1$.

$\alpha_F < 1$, the trivial solution $T = \bar{T}$ is not a solution of (15). It is easy to show that for α_F slightly smaller than 1, there exists two solutions at both sides of μ_c, one of which is positive and the other which is negative. Therefore, the transcritical bifurcation breaks up, as illustrated for the specific case in Fig. 8b, where $\bar{\tau}_{ext}$ is chosen as $\bar{\tau}_{obs}/4$. With decreasing α_F, the upper warm branch moves to larger values of μ. This is the same qualitative behavior as in the spatially dependent model (Fig. 5a). The cold branch is continuously deformed from the flux-corrected case to the coupled climatology case ($\alpha_F = 0.0$, Fig. 8a). The warm branch has completely disappeared in this case, leaving a unique solution in the fully coupled case. This can easily be seen from the value of the coupling at which the upwelling–downwelling switch occurs; namely, $\mu = -[\bar{\tau}_{ext} + \alpha_F(\bar{\tau}_{obs} - \bar{\tau}_{ext})][\alpha_F(T_0 - \bar{T})]^{-1}$. This moves to infinity as $\alpha_F \to 0$, while the solution with upwelling

($w > 0$) on the upper branch approaches the constant temperature state ($T = T_0$).

c. *Summary of typical behavior in the fully coupled case*

A detailed analysis of the solutions of the toy model in the fully coupled case ($\alpha_F = 0$) is presented in the appendix. The essential results are that for realistic situations, with easterly $\bar{\tau}_{ext}$, a single solution branch exists yielding only one stationary state at each value of the coupling. At $\mu = 0$, the temperature is slightly colder than the surface-flux equilibrium temperature T_0 due to slight upwelling $w_0 > 0$ created by the externally forced easterlies $\bar{\tau}_{ext} < 0$ (and by additional entrainment into the mixed layer independent of mean wind, if included). As coupling is increased, a combination of upwelling and thermocline feedbacks causes the temperature to drop and easterlies to increase (a strengthening of the "cold tongue"). The solution structure is the same as in Fig. A1a in the appendix. For the example case (values listed in Table 2), this type of solution is shown in Fig. 9 for $\bar{\tau}_{ext} = -0.2$ and -0.1. Changing ocean model parameters gives varying quantitative results, but the qualitative behavior remains the same (topologically equivalent).

d. *Analysis of symmetry breaking in the fully coupled case*

To explain the spontaneous symmetry breaking as observed in Fig. 5c, we look at what happens if the magnitude of $\bar{\tau}_{ext}$ (and thereby w_0, that is, assuming no additional entrainment) is reduced to zero. The line labeled "0.0" in Fig. 9 shows this case, which differs from the normal situation in two aspects. The more important feature is that the trivial solution (i.e., surface-flux equilibrium unaffected by ocean dynamics), which exists for all μ in this special case, goes unstable (point labeled B). A cold branch arises by spontaneous symmetry breaking, as in Fig. 5c, and at a somewhat higher coupling, comes to resemble the cold branch of the realistic case. Thus, in this limit there is indeed a multiplicity of solutions, but only the cold branch is stable over most of the domain. This case is conceptually important because it suggests that the cold-tongue–warm-pool contrast could generate itself even in the absence of external symmetry breaking. Quantitative discussion of this is addressed in Part II.

The second feature of the $\bar{\tau}_{ext} = 0$ solution in Fig. 9 is that a limit point occurs near $\mu = 0.1$, so the cold branch produces two, rather than one, stationary points in addition to the trivial branch over a very small range of μ. This behavior depends on the relative importance of upwelling and thermocline feedbacks and is restricted enough that it is unlikely to be important.

The structure for $w_0 \to 0$ can be easily understood from the general analysis given in the appendix. In this limit, $h = \mu T'$ and the equation determining the solutions is Eq. (A3) for μ larger than μ_A, the value of μ at point A (where $h = h_2$) in Fig. 9, and Eq. (A5) along the branch from A to B. The solutions of (A5) for $w_0 = 0$ are $T' = 0$ and

$$T' = \left[\frac{\epsilon_T}{\mu\delta_s} - (\gamma h_2 + T_0 - T_2)\right](1 - \gamma\mu)^{-1}. \quad (16)$$

This second root is exactly allowed from A to B (in Fig. 9); the solution (16) is not allowed for $T' > 0$ because then (through the upwelling–downwelling nonlinearity) there is total downwelling. The bifurcation from the trivial solution at B occurs for $\mu_B = \epsilon_T[\delta_s(\gamma h_2 + T_0 - T_2)]^{-1}$ and slopes toward smaller μ as in Fig. 9 when $\delta_s < \gamma\epsilon_T(\gamma h_2 + T_0 - T_2)^{-1}$. For larger δ_s, the branch between A and B could have T decreasing with increasing μ, and these would be only a single stationary point in addition to the trivial one. In either case, the trivial solution is unstable beyond μ_B.

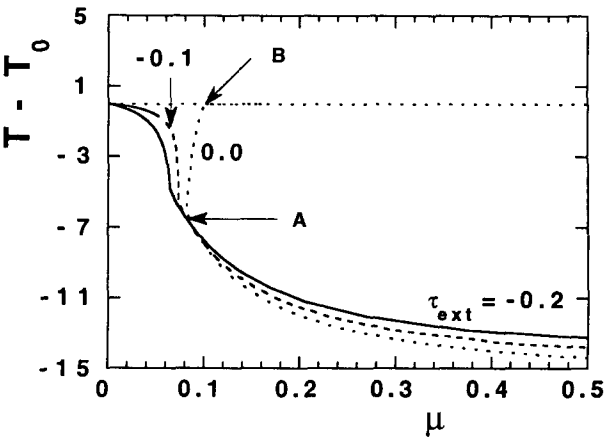

FIG. 9. Bifurcation picture for the "toy" model for the fully coupled case for several values of $\bar{\tau}_{ext}$ (−0.2, −0.1 and 0.0), showing how the symmetry breaking structure of Fig. 5c arises.

5. Discussion

Coupled ocean–atmosphere models of various levels of complexity, from coupled GCMs to toy models, use flux-correction techniques to artificially construct a known climatological state (the term flux correction is applied to all such techniques, even though in simple models the procedure may not explicitly involve modification of climatological fluxes). We have addressed two main points: 1) Flux correction can have a drastic impact on the bifurcation structure of coupled models of the tropical Pacific, as compared with the case where the climatology is itself simulated as a coupled phenomenon. However, the aspects of the problem for which the flux-corrected situation is problematic can be distinguished from those where it is useful. 2) The

tropical example serves to point out that simple considerations from the imperfection theory (e.g., Iooss and Joseph 1990) can be used to place some caveats on the use of flux-correction techniques more generally.

Early discussion of the ENSO phenomenon was often phrased in terms of multiple stationary states, thought of as a warm "El Niño" state and a cold counterpart sometimes referred to as "La Niña" (Philander 1985), and some of the early ENSO models had such multiple states artificially built in (McCreary and Anderson 1984). Subsequent modeling (e.g., Zebiak and Cane 1987; Battisti and Hirst 1989) and observational work (e.g., Rasmusson et al. 1990) has lead to a consensus view of ENSO as an essentially cyclic phenomenon. It has, however, been difficult to lay the notion of multiple stationary states entirely to rest because these are in fact found in some tropical coupled models in some flow regimes. Even when the first bifurcation from the climatology is a Hopf bifurcation with an interannual period and ENSO-like characteristics, it is common for ENSO models to exhibit stationary bifurcations from the constructed climate state at higher coupling. For instance, the point-coupling model of Suarez and Schopf (1988), which was intended to explain cyclic behavior, was originally used in a regime that has unstable stationary states in addition to the limit cycle. Battisti and Hirst (1989) pointed out that a better estimate of the parameters suggested that the regime below the stationary bifurcation was more appropriate; the presence of these states in this model nonetheless continues to attract attention (McCreary and Anderson 1991; Wu et al. 1993; Wakata and Sarachik 1994) and has sometimes lead to terminological confusion, such as the use of the term "switching," even in models that do not possess multiple equilibria (Wakata and Sarachik 1991). Multiple stationary states are noted in intermediate coupled models in Hao et al. (1993) and Zebiak and Cane (1987). They are explored carefully in DN since even when they are unstable, and thus difficult to infer from time integration, they can exert considerable influence on the evolution of the flow. Recently, Wu et al. (1993), examining the influence of external forcing on an ENSO model, carefully devoted half the paper to a regime with multiple stationary states, and Wakata and Sarachik (1994) focus on multiple equilibria in their model. An example of multiple stationary states influencing the ENSO-like cycle of a hybrid coupled model (HCM) was used to indicate in DN that such effects are not restricted to the simple and intermediate models, but can occur with the full nonlinearity of an ocean GCM, and that the intermediate models can explain the HCM results rather well.

We are now in a position to state that *the existence of multiple equilibria in these models is an artifact of the flux correction* and does not correspond to any structure that is likely to occur in the fully coupled tropical system. We show how this occurs both in a stripped-down intermediate model, where effects of changing spatial structure in the coupled climatology are included and whose behavior closely resembles the Zebiak and Cane (1987) model, and in a point coupling model, whose stationary solutions encompass those that would be found in the Suarez and Schopf (1988), Battisti and Hirst (1989), and Münnich et al. (1991) models, but which includes more general physics in order to mimic the results of intermediate and hybrid coupled models. The artificial production of stationary solutions occurs as follows: the flux correction places a restriction on the system such that the trivial solution, in terms of anomalous variables, exists independent of the model parameters. For instance, suppose a pair of models are coupled with flux correction for several different values of specified parameters (which might include mixing coefficients, etc.). Even if the parameters are such that there is no possibility of maintaining a reasonable cold tongue in the fully coupled case, a reference state resembling observations is still obtained when flux correction is used. Modifications to this stationary state can thus occur only via codimension-1 bifurcations (transcritical/Hopf). The additional stationary branches that arise in these models do so generically as transcritical bifurcations. [Suarez and Schopf (1988) and Battisti and Hirst (1989) obtained pitchfork bifurcations because they excluded quadratic terms from the nonlinearity, but since the full system has no internal symmetry, this is deformed into a transcritical bifurcation.] Transcritical bifurcations are not robust to perturbations of the vector field (see, e.g., Iooss and Joseph 1990), so these must break up when the conditions imposed by flux correction are relaxed and the trivial solution ceases to exist. If the change to the system could be regarded as a small perturbation, multiple stationary points could continue to exist by having two unconnected solution branches, at least one of which has a saddle node bifurcation (this configuration can, of course, be seen when an artificial parameter is used to move gradually from the flux-corrected case to a non-flux-corrected case). However, for the particular physical situation relevant to the tropical coupled climatology, one of the branches (the warm branch) moves away to infinity when the flux correction is removed completely. This leaves a single stationary branch that evolves nonlinearly as a function of model parameters.

From a physical point of view, this occurs because the coupled processes involve dynamical redistribution of warm and cold water, with the winds depending on the resulting pattern of SST. In the non-flux-corrected case, the resulting circulation can make the equatorial SST colder by upwelling colder water from below, and feedbacks between the SST and wind can rearrange the pattern of SST, but processes due to the large-scale dynamics do not tend to make SST significantly warmer than would occur in a state without dynamical effects. The coupled feedbacks in the model climatology

thus tend to produce an equatorial cold tongue, which might be too weak or too strong, or might be of a different shape than observed (and which might or might not be unstable to ENSO-like time-dependent variability), but which is almost always a unique stationary solution (see appendix for exotic exceptions). In the flux-corrected case, there is an artificial solution with a certain strength of the equatorial cold tongue. If model parameters, such as coupling strength, are such that coupled feedbacks would normally create, for instance, a stronger cold tongue, the flux correction prevents this from occurring. Instead of gradually increasing the strength of the cold tongue as coupling is increased, no change can occur until the feedbacks are strong enough to create a stationary instability and, thus, bifurcating stationary branches. The latter are constrained to occur on both sides of the flux-corrected solution, so in addition to a cold branch that resembles the solution for the fully coupled case, a spurious warm branch must appear.

The processes for linear instability of the flux-corrected solutions are those familiar from the discussion of ENSO feedbacks and are equivalent for the warm and cold sides, although asymmetry in the nonlinearity results in differences between the warm and cold branches: a cold (warm) anomaly results in easterly (westerly) wind anomalies, giving increased (decreased) upwelling and a shallower (deeper) thermocline. These feedbacks are physically reasonable and are precisely the ones that are correctly producing the deepened cold tongue in the fully coupled case (or approximations to this in the flux-corrected case) on the cold branch. The erroneous configuration arises, roughly speaking, because the presence of the artificial flux-corrected state, with anomalies defined with respect to it, forces the feedbacks to create a third branch instead of modifying a single branch.

Although only stationary solutions have been explicitly discussed, we can invoke standard results for bifurcations of a solution with periodic coefficients to consider what must happen in the case where the flux-corrected solution contains a seasonal cycle. Bifurcations with the fundamental period (i.e., unstable solutions with one-yr period) behave in the same manner as the transcritical bifurcations discussed here (Iooss and Joseph 1990, chapter IX.19). The same qualitative behavior found here will thus apply in the presence of the seasonal cycle: multiple solutions with an annual period that could occur in the presence of flux correction will disappear when the flux correction is removed.

A similar qualitative argument can be made to provide good news regarding the ENSO cycles of models with flux correction, based on the fact that Hopf bifurcations are robust to perturbations of this sort. Since most model ENSO cycles arise by supercritical Hopf bifurcation, the use of flux correction will not adversely affect these as long as no spurious stationary branches interfere with the cycle. There are large parts of parameter space where this condition can be met (DN), especially for coupling values that are not too far above the Hopf bifurcation. However, any cases that appear as if the time-dependent behavior might involve interaction with an unstable stationary point [e.g., some of the parameter regimes of the Zebiak and Cane (1987) model and related models, high-coupling behavior in Münnich et al. (1991), the relaxation oscillations found in Hao et al. (1993) and DN] should be interpreted with caution. The sensitivity of the period of the Hopf bifurcation to increases in coupling can also be expected to be less in the non-flux-corrected case than with flux correction. The most unstable modes of the flux-corrected state tend to become stationary at high coupling where local feedbacks dominate over wave dynamical processes (Jin and Neelin 1993a,b). In the region near these singularities, the frequency on the oscillatory side goes quite rapidly from a finite value to zero; in the non-flux-corrected case, these codimension-two bifurcations will not occur. Examination of the linear, stationary growing modes can still be worthwhile for purposes of understanding. They often provide simpler prototypes to examine how the spatial structure of coupled modes is determined and how coupled feedbacks work, as long as one bears in mind that not all the branches of stationary states associated with these are realistic. In particular, these modes can likely be used to understand how the cold tongue intensifies since we have noted cases where the spatial structure of the cold branch in the flux-corrected case corresponds well to the fully coupled case (provided the warm branch is ignored).

The above discussion focuses on the qualitative impacts of flux-correction on the topological structure of the attractors of the tropical coupled system. There are also some effects of flux correction that can negatively impact interannual variability that are quite separate from those discussed here; for instance, if winds obtained with an AGCM are weak, the strength of the flux-corrected cold tongue tends to inhibit interannual variability (Neelin et al. 1992; Latif et al. 1988). However, there are also many quantitative effects of errors in a fully coupled model climatology that can adversely affect the quality of simulation of interannual variability and make flux correction an attractive option, especially for models of intermediate complexity or for situations where the climatology is even harder to simulate correctly than in the tropical case, such as for the global climate problem. The principal caveat that can be extended from the tropical example is that when flux correction is used, any result involving multiple stationary states (e.g., Bryan 1986; Manabe and Stouffer 1988; Weaver et al. 1991) should be viewed with caution. This holds in general because the breakup of stationary bifurcations from the flux-corrected state depends only on generic properties. Multiple stationary states can potentially persist (with topology different from the flux-corrected case) but should be distrusted

until the physics have been examined in a non-flux-corrected context. The methods employed here can potentially be used to generalize and provide a structural context for quantitative examination of the flux-correction problem for the oceanic thermocline circulation, such as Zhang et al. (1993), Tziperman et al. (1994), and Marotzke and Stone (1994).

For the tropical case, none of the means of obtaining multiple stationary states examined here is realistic for the coupled climatology of the tropical Pacific (although individual branches may have some conceptual value in particular cases). While we cannot exclude the possibility of some more exotic mechanism producing multiple tropical equilibria, the results show definitively that those produced by existing models are spurious, and very strongly reinforce the conclusion that multiple equilibria play no role in ENSO.

Acknowledgments. This work was supported in part by National Science Foundation Grant ATM-9215090 (JDN). This work was initiated during a visit of HD to UCLA in November 1992, finished during a second visit in November 1993, and submitted during a visit by JDN to M.I.T. under support from the Houghton Lectureship. Support for the first visit of HD was obtained through a travel grant from the Nederlandse Organisatie voor Wetenschappelijk Onderzoek (Netherlands Organization for Scientific Research, NWO), and for the second through National Science Foundation Grant ATM-9158294. All computations were performed on the CRAY Y-MP at the Academic Computer Centre (SARA), Amsterdam, the Netherlands. Use of these computing facilities was sponsored by the Stichting Nationale Supercomputer Faciliteiten (National Computing Facilities Foundation, NCF) with financial support from the Nederlandse Organisatie voor Wetenschappelijk Onderzoek. One of authors (HD) thanks Will de Ruijter (I.M.A.U) for much encouragement and support.

APPENDIX

Detailed Analysis of the "Toy" Model in the Fully Coupled Case

In the fully coupled case ($\alpha_F = 0$), the equation for the temperature departure from the surface heat flux equilibrium value $T' = T - T_0$ becomes

$$\mathscr{H}(w_0 - \mu\delta_s T')(w_0 - \mu\delta_s T')[T' + T_0 - T_s(h)] + \mathscr{H}(-w_0 + \mu\delta_s T')(\mu\delta_s T' - w_0)(T' + T_0 - T_N) + \epsilon_T T' = 0 \quad \text{(A1a)}$$

$$h = \bar{h}_{\text{ext}} + \mu T'. \quad \text{(A1b)}$$

For simplicity, we first consider w_0 to be independent of $\bar{\tau}_{\text{ext}}$. In general, w_0 will have a part driven by the external winds and possibly an additional positive contribution corresponding to an entrainment velocity into the mixed layer. The connection between w_0 and $\bar{\tau}_{\text{ext}}$ is made after presenting all cases of model solutions.

For climatological upwelling ($w_0 > 0$), the solution structure is divided into three different regions:

case (a) $\bar{\tau}_{\text{ext}} < h_2$.

The solution for $\mu = 0$ is

$$T' = \frac{w_0(T_2 - T_0)}{w_0 + \epsilon_T} < 0. \quad \text{(A2)}$$

For $\mu \neq 0$, there are two possibilities (in the case of total upwelling):

case (a1) $w_0 > \mu\delta_s T'$ and $h < h_2$; case (a2) $w_0 > \mu\delta_s T'$ and $h > h_2$.

In case (a1) the solutions are determined by

$$(w_0 - \mu\delta_s T')[T' - (T_2 - T_0)] + \epsilon_T T' = 0. \quad \text{(A3)}$$

For $\delta_s = 0$, the solution (A2) is the only solution for all μ. For $\delta_s \neq 0$, Eq. (A3) has two roots, $T' = \phi \pm \chi^{1/2}$, with $\chi > 0$. The root $\phi - \chi^{1/2}$ is the continuation of the $\mu = 0$ solution. The other (positive) root (which becomes unbounded for $\mu \to 0$) does not satisfy the inequality $w_0 > \mu\delta_s T'$ and hence it has to be rejected. The solutions for case (a2) form part of the solutions of cases (b) and (c) below:

case (b) $h_2 < \bar{\tau}_{\text{ext}} < h_1$.

Let $\beta_1 = \gamma(h_2 - \bar{\tau}_{\text{ext}}) + T_0 - T_2$ and consequently $\beta_1 \geqslant T_0 - T_1 \geqslant 0$; then the solution at $\mu = 0$ is given by

$$T' = \frac{-\beta_1 w_0}{w_0 + \epsilon_T} \quad (\leqslant 0 \text{ if } T_1 = T_0). \quad \text{(A4)}$$

For $w_0 > \mu\delta_s T'$, and if $h < h_2$, the solution is given by case (a1). Hence, there are two extra possibilities:

case (b1) $h_2 < h < h_1$; case (b2) $h > h_1$.

In case (b1), the solution is determined by

$$(w_0 - \mu\delta_s T')[T'(1 - \gamma\mu) + \beta_1] + \epsilon_T T' = 0. \quad \text{(A5)}$$

For $\delta_s = 0$, the solution is given by

$$T' = \frac{-\beta_1 w_0}{w_0(1 - \gamma\mu) + \epsilon_T}, \quad \text{(A6)}$$

which has a vertical asymptote at $\mu_c = (\epsilon_T + w_0)/(\gamma w_0)$. For $\mu > \mu_c$, the solution T' is positive and for $\mu < \mu_c$ it is negative. Note that both branches of the solution only have validity within the conditions defined by (b1). For $\delta_s \neq 0$, the quadratic equation (A5) has two real roots if $\mu < \gamma^{-1}$; one of these roots is positive and the other is negative. At $\mu = \gamma^{-1}$, the solution is given by

$$T' = \frac{\beta_1 w_0}{\mu\delta_s\beta_1 - \epsilon_T}, \quad \text{(A7)}$$

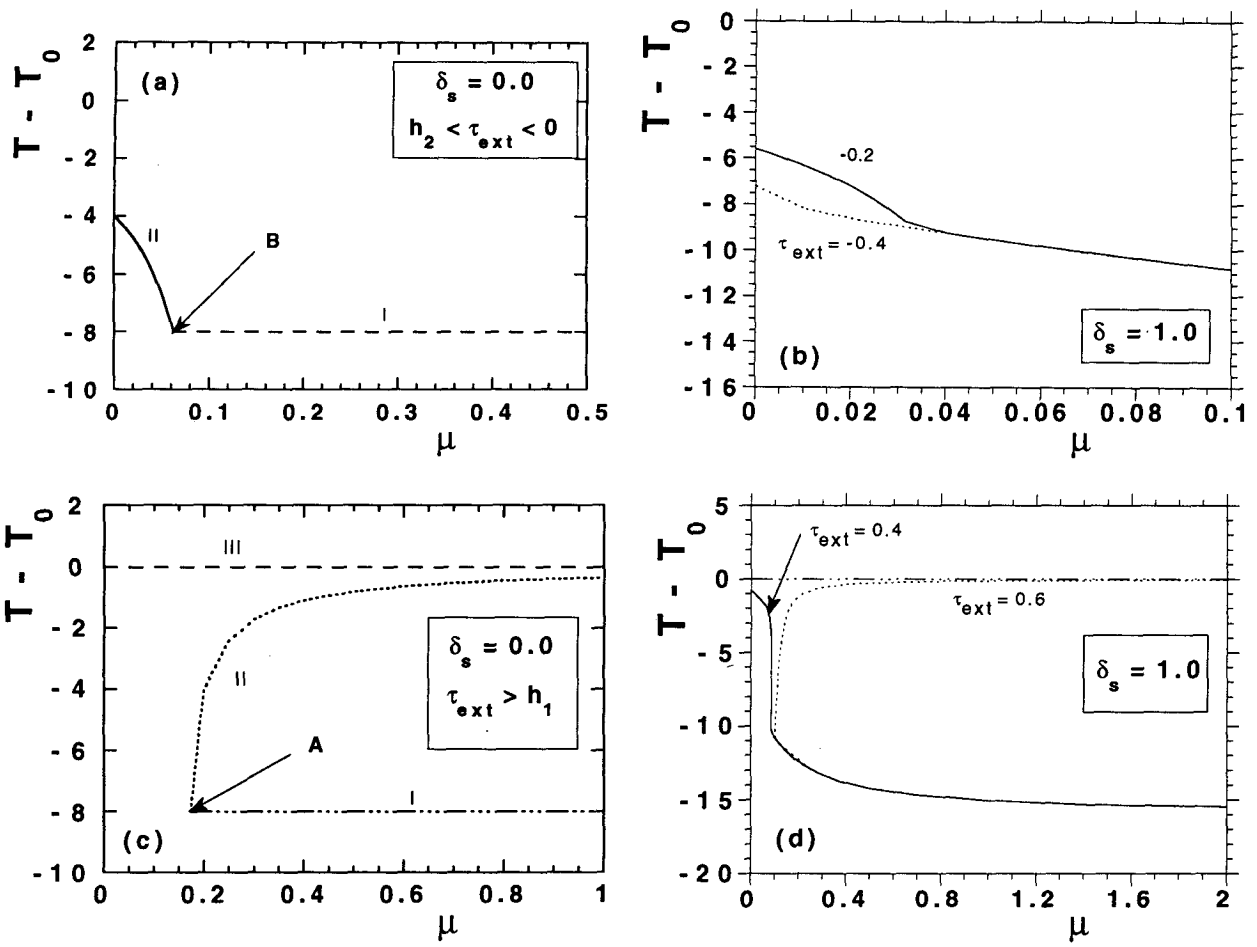

FIG. A1. Bifurcation diagrams for several values of $\bar{\tau}_{ext}$ and δ_s for the "toy" model. (a) $\delta_s = 0.0$, $h_2 \leqslant \bar{\tau}_{ext} \leqslant 0$; (b) $\delta_s = 1.0$, $\bar{\tau}_{ext} = -0.4, -0.2$; (c) $\delta_s = 0.0$, $\bar{\tau}_{ext} \geqslant h_1$; (d) $\delta_s = 1.0$, $\bar{\tau}_{ext} = 0.4, 0.6$.

and for $\mu > \gamma^{-1}$, the solutions become complex conjugate and thus have to be rejected. Case (b2) is part of the solution of the following case, (c):

case (c) $\bar{\tau}_{ext} > h_1$.

Now for $\mu = 0$, the solution is given by

$$T' = \frac{w_0(T_1 - T_0)}{w_0 + \epsilon_T} \quad (\leqslant 0 \text{ for } T_1 - T_0 \leqslant 0). \quad \text{(A8)}$$

For $\mu \neq 0$, if h becomes smaller than h_1, the solution structure of case (b1) applies. The only remaining case we have to consider is

case (c1) $h > h_1$.

The solution structure is then determined by

$$(w_0 - \mu\delta_s T')[T' - (T_1 - T_0)] + \epsilon_T T' = 0. \quad \text{(A9)}$$

For $T_1 = T_0$, the only solution is $T' = 0$ for all values of μ, because for the other solution (if $\delta_s \neq 0$) $\mu\delta_s T' = w_0 + \epsilon_T > w_0$. This completes the possible solution structures of the "toy" model for constant $w_0 > 0$.

For climatological downwelling ($w_0 < 0$), the structure of solutions is very simple if $T_N = T_0$. There are two possible cases:

case (d1) $w_0 - \mu\delta_s T' > 0$; case (d2) $w_0 - \mu\delta_s T' < 0$.

Case (d1) corresponds to a solution of previous cases (a)–(c). In case (d2), the equation determining the steady states is

$$(\mu\delta_s T' - w_0)T' + \epsilon_T T' = 0. \quad \text{(A10)}$$

The trivial solution is always a solution while the other root must be rejected (since $\mu\delta_s T' = w_0 - \epsilon_T < w_0$). In short, there is net downwelling, so the upwelling–downwelling nonlinearity only generates the zero anomaly solution.

Having presented all possible cases, we now discuss them in physical terms. Climatologically relevant cases are obtained only for $\bar{\tau}_{ext} \leqslant 0$, since in reality the global Hadley circulation contributes a significant external easterly stress. Realistic solutions for the Pacific basin must come from among cases (a) and (b). We consider

first $\delta_s = 0$, in which case the solution structure is quite simple (see Fig. A1a). Suppose $h_2 \leq \bar{\tau}_{ext} \leq 0$; then for values of μ up to μ_B, $h > h_2$ (class b). For larger values of μ, the branch I [case (a1)] is the only solution. Finally, if $\bar{\tau}_{ext}$ decreases down to h_2, point B in Fig. A1a shifts to $\mu = 0$ because $\beta_1 \to T_2 - T_0$. For $\delta_s \neq 0$, the structure is similar and shown for a particular case (parameters in Table 2) for several values of $\bar{\tau}_{ext}$ in Fig. A1b.

To see whether we can push the system so far as to get a multiplicity of steady states in some regimes, we now consider some cases that are not climatologically realistic; for instance, with $\bar{\tau}_{ext} \geq h1$, strong westerlies. Again, $\delta_s = 0$ is considered first. For $\bar{\tau}_{ext} > h_1$, there are three solution branches as in Fig. A1c. The trivial solution (III) is a solution for all μ as described in case (c1). However, there exist also solutions for which $h < h_1$—for example, case (b1) (the curve II); note that if $\bar{\tau}_{ext} > h_1$, then $\beta_1 < 0$. There is another branch II that is rejected because $h > h_1$; the branch II shown satisfies the conditions of (b1) for $\mu > \mu_A$. Another solution exists from case (a1). This solution must be rejected for $\mu < \mu_A$ because then $h > h_2$. In summary, for $\mu < \mu_A$ there is only one solution, while for $\mu > \mu_A$ there are three solutions.

For $\delta_s \neq 0$, similar features appear, although the detailed analysis is more involved (but elementary). In Fig. A1d we show examples of the structures of the steady states for $\delta_s = 1.0$ and several values of $\bar{\tau}_{ext}$. Again it is seen that as $\bar{\tau}_{ext}$ becomes larger than h_1, there is only one solution for small μ (i.e., the trivial one) and three for larger μ.

Although not climatologically realizable for the Pacific, these examples do, in fact, give insight into the processes that prevent or permit multiple states in the tropical climatology. Because the horizontal and vertical advection by ocean dynamical processes cannot produce SSTs warmer than the upper temperature range given by the surface heat flux equilibrium temperature, the amount of warming of SST that can be produced by westerly winds is bounded. In surface heat-flux equilibrium, the ocean regions are not much different than neighboring land areas, so essentially no temperature gradients required to produce Walker circulation winds can be produced by land–sea contrast either. Once upwelling is shut off and the temperature gradients are flat, no additional warming can occur and thus no feedback can occur that could maintain westerly winds. Thus, when the external wind stress is easterly, coupled feedbacks tend to increase the easterlies and cannot generate any additional warm state with westerlies. On the other hand, if the climatology were driven by external westerlies, leaving temperatures warm along the equator due to lack of upwelling, one could obtain additional self-consistent cold states because anomalous easterlies may induce upwelling of cold water. The contrast between cold water in ocean regions and relatively warm land can maintain easterlies, which in turn can maintain the cold water. The temperature is in this case bounded through the bound on the subsurface temperature. It is thus not physically inconceivable to create a tropical ocean basin that could genuinely have multiple equilibria. The physics and the topology of the stationary branches would, however, be significantly different from the spurious equilibria in flux-corrected models, on the one hand, and from the climatologically realistic case, on the other. It is also possible to find very localized regions of parameter space that have multiple equilibria associated with saddle node (hysteresis) bifurcations (e.g., dashed curve in Fig. 9) in non-flux-corrected cases. These have a different, more robust topology than the spurious multiple equilibria generated by flux correction but occur only in very limited circumstances.

REFERENCES

Battisti, D. S., and A. C. Hirst, 1989: Interannual variability in a tropical atmosphere–ocean model: Influence of the basic state, ocean geometry, and nonlinearity. *J. Atmos. Sci.*, **46**, 1687–1712.

Bjerknes, J., 1969: Atmospheric teleconnections from the equatorial Pacific. *Mon. Wea. Rev.*, **97**, 163–172.

Bryan, F., 1986: High-latitude salinity effects and interhemispheric thermohaline circulations. *Nature*, **323**, 301–304.

Dijkstra, H. A., and J. D. Neelin, 1995a: On the attractors of an intermediate coupled equatorial ocean-atmosphere model. *Dyn. Atm. Oceans*, in press.

——, and ——, 1995b: Ocean–atmosphere interaction and the tropical climatology. Part II: Why the Pacific cold tongue is in the east. *J. Climate*, **8**, 1343–1359.

Endoh, M., T. Tokioka, and T. Nagai, 1991: Tropical Pacific sea surface temperature variations in a coupled atmosphere–ocean general circulation model. *J. Mar. Sys.*, **1**, 293–298.

Gates, W. L., Y. J. Han, and M. E. Schlesinger, 1985: The global climate simulated by a coupled atmosphere–ocean general circulation model—preliminary results. *Coupled Ocean–Atmosphere Models*, Elsevier Oceanogr. Ser. 40. J. C. J. Nihoul, Ed., 131–151.

Gent, P. R., and J. J. Tribbia, 1993: Simulation and predictability in a coupled TOGA model. *J. Climate*, **6**, 1843–1858.

Ghil, M., and S. Childress, 1987: *Topics in Geophysical Fluid Dynamics: Atmospheric Dynamics, Dynamo Theory, and Climate Dynamics*. Springer-Verlag, 485 pp.

Gordon, C., 1989: Tropical ocean–atmosphere interactions in a coupled model. *Phil. Trans. Roy. Soc. London*, **A329**, 207–223.

Hao, Z., J. D. Neelin, and F. Jin, 1993: Nonlinear tropical air–sea interaction in the fast wave limit. *J. Climate*, **6**, 1523–1544.

Iooss, G., and D. D. Joseph, 1990: *Elementary Stability and Bifurcation Theory*. Springer-Verlag, 324 pp.

Jin, F.-F., and J. D. Neelin, 1993a: Modes of interannual tropical ocean–atmosphere interaction—a unified view. Part I: Numerical results. *J. Atmos. Sci.*, **50**, 3477–3503.

——, and ——, 1993b: Modes of interannual tropical ocean–atmosphere interaction—a unified view. Part III: Analytical results in fully coupled cases. *J. Atmos. Sci.*, **50**, 3523–3540.

Keller, H. B., 1977: Numerical solution of bifurcation and nonlinear eigenvalue problems. *Applications of Bifurcation Theory*, P. H. Rabinowitz, Ed., Academic Press, 359–383.

Latif, M., J. Biercamp, and H. von Storch, 1988: The response of a coupled ocean–atmosphere general circulation model to wind bursts. *J. Atmos. Sci.*, **45**, 964–979.

——, T. Stockdale, J. Wolff, G. Burgers, E. Maier-Reimer, M. M. Junge, K. Arpe, and L. Bengtsson, 1994: Climatology and variability in the ECHO coupled GCM. *Tellus*, **46A**, 351–366.

Manabe, S., and R. J. Stouffer, 1988: Two stable equilibria of a coupled ocean–atmosphere model. *J. Climate,* **1,** 841–866.

Marotzke, J., and P. H. Stone, 1994: Atmospheric transports, the thermohaline circulation, and flux adjustments in a simple coupled model. Center for Global Change Science, Rep. No. 29, Massachusetts Inst. Tech., 30 pp.

McCreary, J. P., and D. L. T. Anderson, 1984: A simple model of El Niño and the Southern Oscillation. *Mon. Wea. Rev.,* **112,** 934–946.

——, and ——, 1991: An overview of coupled ocean–atmosphere models of El Niño and the Southern Oscillation. *J. Geophys. Res.,* **96,** 3125–3150.

Mechoso, C. R., C.-C. Ma, J. D. Farrara, J. Spahr, and R. W. Moore, 1993: Parallelization and distribution of a coupled atmosphere–ocean general circulation model. *Mon. Wea. Rev.,* **21,** 2062–2076.

Meehl, G. A., 1990: Development of global coupled ocean–atmosphere general circulation models. *Climate Dyn.,* **5,** 19–33.

Mitchell, T. P., and J. M. Wallace, 1992: The annual cycle in equatorial convection and sea surface temperature. *J. Climate,* **5,** 1140–1156.

Münnich, M., M. A. Cane, and S. E. Zebiak, 1991: A study of self-excited oscillations of the tropical ocean–atmosphere system. Part II: Nonlinear cases. *J. Atmos. Sci.,* **48,** 1238–1248.

Nagai, T., T. Tokioka, M. Endoh, and Y. Kitamura, 1992: El Niño–Southern Oscillation simulated in an MRI atmosphere–ocean coupled general circulation model. *J. Climate,* **5,** 1202–1233.

Neelin, J. D., and F.-F. Jin, 1993: Modes of interannual tropical ocean–atmosphere interaction—a unified view. Part II: Analytical results in the weak-coupling limit. *J. Atmos. Sci.,* **50,** 3504–3522.

——, M. Latif, and Coauthors, 1992: Tropical air–sea interaction in general circulation models. *Climate Dyn.,* **7,** 73–104.

Philander, S. G. H., 1985: El Niño and La Niña. *J. Atmos. Sci.,* **42,** 2652–2662.

——, and Y. Chao, 1991: On the contrast between the seasonal cycles of the equatorial Atlantic and Pacific Oceans. *J. Phys. Oceanogr.,* **21,** 1399–1406.

——, R. C. Pacanowski, N. C. Lau, and M. J. Nath, 1992: Simulation of ENSO with a global atmospheric GCM coupled to a high-resolution, tropical Pacific Ocean GCM. *J. Climate,* **5,** 308–329.

Rasmusson, E. M., X. Wang, and C. F. Roplewski, 1990: The biennial component of ENSO variability. *J. Mar. Sys.,* **1,** 71–96.

Sausen, R., K. Barthels, and K. Hasselmann, 1988: Coupled ocean–atmosphere models with flux correction. *Climate Dyn.,* **2,** 154–163.

Sperber, K. R., S. Hameed, W. L. Gates, and G. L. Potter, 1987: Southern Oscillation simulated in a global climate model. *Nature,* **329,** 140–142.

Suarez, M. J., and P. Schopf, 1988: A delayed action oscillator for ENSO. *J. Atmos. Sci.,* **45,** 3283–3287.

Tziperman, E., J. R. Toggweiler, Y. Feliks, and K. Bryan, 1994: Instability of the thermohaline circulation with respect to mixed boundary conditions: Is it really a problem for realistic models? *J. Phys. Oceanogr.,* **24,** 217–232.

Wakata, Y., and E. S. Sarachik, 1991: Unstable coupled atmosphere–ocean basin modes in the presence of a spatially varying basic state. *J. Atmos. Sci.,* **48,** 2060–2077.

——, and ——, 1994: Nonlinear effects in coupled atmosphere–ocean basin modes. *J. Atmos. Sci.,* **51,** 909–920.

Weaver, A. J., E. S. Sarachik, and J. Marotzke, 1991: Freshwater flux forcing of decadal and interdecadal oceanic variability. *Nature,* **353,** 836–838.

Wu, D.-H., D. L. T. Anderson, and M. K. Davey, 1993: ENSO variability and external impacts. *J. Climate,* **6,** 1703–1717.

Zebiak, S. E., and M. A. Cane, 1987: A model El Niño–Southern Oscillation. *Mon. Wea. Rev.,* **115,** 2262–2278.

Zhang, S., R. J. Greatbatch, and C. A. Lin, 1993: A reexamination of the polar halocline catastrophe and implications for coupled ocean–atmosphere modeling. *J. Phys. Oceanogr.,* **23,** 287–299.